

# UC Berkeley

## UC Berkeley Previously Published Works

### Title

Resolution of a discrepancy in the  $\gamma$ -ray emission probability from the  $\beta$  decay of Ceg137

### Permalink

<https://escholarship.org/uc/item/94b8p7fx>

### Journal

Physical Review C, 101(6)

### ISSN

2469-9985

### Authors

Basunia, MS  
Morrell, JT  
Uddin, MS  
[et al.](#)

### Publication Date

2020-06-01

### DOI

10.1103/physrevc.101.064619

Peer reviewed

Resolution of a discrepancy in the  $\gamma$ -ray emission probability from the  $\beta$  decay of  $^{137}\text{Ce}^g$ M. S. Basunia<sup>1</sup>, J. T. Morrell<sup>2</sup>, M. S. Uddin<sup>3</sup>, A. S. Voyles<sup>1,2</sup>, C. D. Nesaraja<sup>4</sup>, L. A. Bernstein<sup>1,2</sup>, E. Browne<sup>1</sup>, M. J. Martin<sup>4</sup>, and S. M. Qaim<sup>5</sup><sup>1</sup>Nuclear Science Division, Lawrence Berkeley National Laboratory, Berkeley, California 94720, USA<sup>2</sup>Department of Nuclear Engineering, University of California Berkeley, Berkeley, California 94720, USA<sup>3</sup>Tandem Accelerator Facilities, INST, Atomic Energy Research Establishment, Savar, Dhaka, Bangladesh<sup>4</sup>Physics Division, Oak Ridge National Laboratory, Oak Ridge, Tennessee 37831, USA<sup>5</sup>Institut für Neurowissenschaften und Medizin, INM-5:Nuklearchemie, Forschungszentrum Jülich, D-52425 Jülich, Germany

(Received 13 September 2019; revised manuscript received 28 January 2020; accepted 11 May 2020; published 19 June 2020)

We have deduced the emission probability of the 447-keV  $\gamma$  ray from the  $\varepsilon + \beta^+$  decay of  $^{137}\text{Ce}^g$  (9.0 h) relative to that of the 254-keV  $\gamma$  ray from the  $^{137}\text{Ce}^m$  (34.4 h) decay in transient equilibrium. The time-dependent factor in transient equilibrium was applied following the Bateman equation for a radioactive decay chain. The isotope was produced via the  $^{139}\text{La}(p, 3n)^{137}\text{Ce}^{m,g}$  reaction by bombarding  $^{nat}\text{La}$  with a proton beam from the 88-in. cyclotron at Lawrence Berkeley National Laboratory.  $\gamma$ -ray intensities were measured using an HPGe detector. The emission probability for the 447-keV  $\gamma$  ray deduced in this work is 1.21(3) (that is  $1.21 \pm 0.03$ ) per hundred parent decays, which differs significantly from an earlier published value of 2.24(10). We identify the source of this discrepancy to be an incorrect use of the time-dependent factor. Additionally, we have deduced the emission probability of the 504-keV  $\gamma$  ray from the decay of  $^{85}\text{Y}^g$  (2.68 h) relative to that of the 232-keV  $\gamma$  ray from the  $^{85}\text{Sr}^m$  (1.127 h) decay in transient equilibrium. The isotope was produced via the  $^{86}\text{Sr}(p, 2n)^{85}\text{Y}^g$  reaction by bombarding  $^{86}\text{SrCO}_3$  with a proton beam at the same facility. The study confirms the assumption of the time-dependent correction for recommending the emission probability of the 504-keV  $\gamma$  ray in the literature. Our work highlights the importance of explicit description by authors of any time-dependent correction they have made when reporting  $\gamma$ -ray intensities for nuclides in transient equilibrium. The need and significance of accurate and precise decay data of  $^{137}\text{Ce}^g$  and  $^{85}\text{Y}^g$  in basic science and medicine is briefly outlined.

DOI: [10.1103/PhysRevC.101.064619](https://doi.org/10.1103/PhysRevC.101.064619)

## I. INTRODUCTION

$\gamma$ -ray emission probabilities  $P_\gamma$  are basic nuclear data widely used in nuclear research, nuclear engineering, and medical applications. In addition to direct measurement of  $P_\gamma$  with different experimental techniques, such as  $4\pi\beta\gamma$  measurements [1,2] or implantation and subsequent decay of parent nuclides in coincidence [3,4], other measured quantities, like absolute x-ray intensity [5], annihilation radiation [6,7], a complete  $\gamma$ -ray decay scheme [8], etc., have frequently been used to extract the  $\gamma$ -ray emission probabilities. Furthermore, relative  $\gamma$ -ray intensities in secular (parent half-life  $\gg$  daughter half-life) or transient equilibrium (parent half-life  $>$  daughter half-life) have also been used to deduce  $\gamma$ -ray emission probabilities of the daughter/parent radionuclides relative to that of their parent/daughter [2,9]. Some of the implantation and additional decay studies including instrumentation can be found in Refs. [10–15].

Henry *et al.* [9] reported a comprehensive level structure of  $^{137}\text{La}$  populated by the  $\varepsilon + \beta^+$  decay of  $^{137}\text{Ce}^{m+g}$  and proposed  $\%P_\gamma(447) = 2.24(10)$  based on their measured ratio of  $I_\gamma(254)/I_\gamma(447) = 4.91(15)$  in transient equilibrium spectra given in a footnote to their Table I. The relevant  $\gamma$ -ray transitions of the  $^{137}\text{Ce}^m$  isomeric decay and  $^{137}\text{Ce}^g$  decay are

shown in Fig. 1. For a known  $\%P_\gamma$  of  $\sim 11$  for the 254-keV isomeric transition, one can readily find that these two numbers are related directly through their ratio. However, it was not clear whether or not the time-dependent correction for a measurement in transient equilibrium was applied. As a result, in the following decades, the recommended emission probability for the 447-keV  $\gamma$  ray from the  $^{137}\text{Ce}^g$  decay followed a duality, i.e., without or with a consideration of the correction factor. For example, the *Table of Isotopes* (7th edition) [16] recommended  $\%P_\gamma(447) = 2.2(1)$ . Later, Peker [17] and the *Table of Radioactive Isotopes* [18] recommended 2.24(10). However, Peker in the revised evaluation [19] suggested a value of  $\%P_\gamma(447) = 1.78(8)$ , using the time-dependent factor. Since then this value remains nearly the same and in the latest evaluation Browne and Tuli [20] proposed a value of 1.68(6) considering the conversion coefficient data from Kibedi *et al.* [21]. Recently, for the  $^{136}\text{Ce}(n, \gamma)^{137}\text{Ce}^g$  reaction cross-section measurements Torrel and Krane [22] used  $\%P_\gamma(447) = 1.69$ , mentioning that it was determined from their measurement. However, no details are available in the article. During the 23rd Technical Meeting of the International Nuclear Structure and Decay Data (NSDD) Network in Vienna, Austria, April, 2019 [23], the issue was presented for discussion with an opinion to change the  $\%P_\gamma(447)$  value

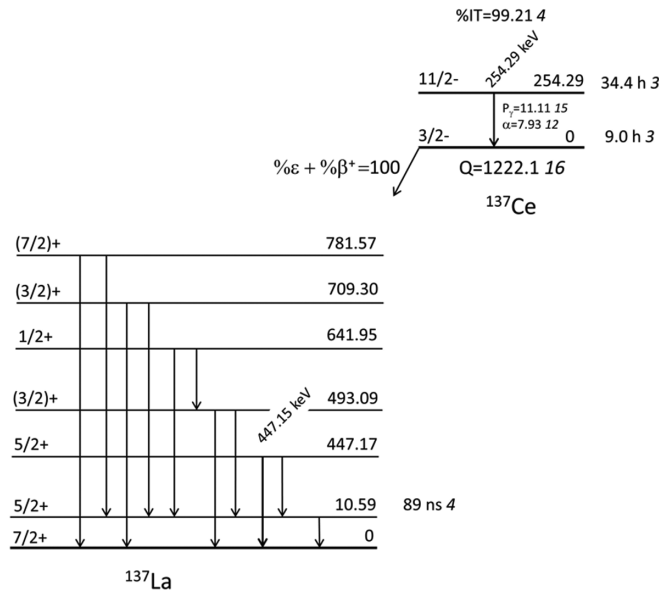


FIG. 1. Partial level scheme (not in scale) showing 254- and 447-keV  $\gamma$  rays from the  $^{137}\text{Ce}^m$  (34.4 h) isomeric decay and the  $^{137}\text{Ce}^g$  (9.0 h) decay, respectively. Detailed decay schemes can be found in Ref. [20].  $\%P_\gamma(254)$  and conversion coefficient  $\alpha$  are also listed.

again to that which was proposed by Henry *et al.* [9]. It may be mentioned here that earlier, Bunting [24] recommended  $\%P_\gamma(447) = 1.4(3)$  based on data from Ref. [25]. All these literature data are presented in Table I (Sec. IV)

To resolve the above mentioned issues, here we report a new measurement for  $\gamma$ -ray emission probability of the 447-keV  $\gamma$  ray from the  $^{137}\text{Ce}^g$  decay and discuss the possible reasons for the discrepancy with the existing literature data. Additionally, we have measured the emission probability of the 504-keV  $\gamma$  ray from the decay of  $^{85}\text{Y}^g$ . The main motivation for the study of the  $^{85}\text{Y}^g$  decay was to verify whether the reported relative intensity of the 232-keV  $\gamma$  ray from the  $^{85}\text{Sr}^m$  decay in Ref. [6], in transient equilibrium with  $^{85}\text{Y}^g$ , was corrected or not for the time-dependent factor.

Accurate and precise  $\gamma$ -ray emission probabilities of  $^{137}\text{Ce}^g$  and  $^{85}\text{Y}^g$  are needed to determine the absolute activity, commonly used for nuclear reaction cross section measurements by activation technique. Isomeric and ground state pairs of  $^{137}\text{Ce}^{m,g}$  and  $^{85}\text{Y}^{m,g}$  having suitable lifetime make them attractive for studying the distribution of spin in excited nuclear states via activation technique [26–28]. The cross section data yielding the relative population of the isomeric state with respect to the ground state have long been used for studying the angular momentum effects in nuclear reactions, spin dependence of the nuclear level density, and testing of nuclear reaction models [29–32]. Also cross section data involving  $^{137}\text{Ce}^{m,g}$  and  $^{85}\text{Y}^{m,g}$  products are important for nucleosynthesis studies of elemental evolution in a stellar environment. These studies use an extensive network of nuclear reactions, of which cross section data for different nuclear reaction channels are important. Stable isotopes in the nuclear chart above iron are classified as *s*, *r*, and *p* nuclei depending upon their nucleosynthesis production process.

The *s* isotopes are produced by the slow (*s*) neutron capture process in stellar environments of helium burning, where beta decay usually occurs between subsequent captures of neutrons due to a moderate density of neutrons. The stable isotopes at the valley of stability in the nuclear chart are considered as being produced through the *s* process. On the other hand, the *r* isotopes are produced in high density neutron environments resulting from explosive stars and are located in the neutron rich side in the nuclear chart. The *p* nuclei [33], which are basically proton rich nuclei in the nuclear chart, have been identified to be produced through a sequence of photodisintegration processes starting from some preexisting seed nuclei [34]. During supernovae explosions,  $\gamma$  rays are energetic enough to initiate subsequent neutron knockout through the  $(\gamma, n)$  reaction on the *s*- and *r*-processed seed nuclei. With the increased neutron separation energies in consecutive compound nuclei, a competing  $(\gamma, p)$  photodisintegration process becomes important [35]. For experimental cross section measurements, however, the common practice is to measure the inverse reaction, for example  $(n, \gamma)$  or  $(p, \gamma)$ , in the laboratory and to extract the cross section for the actual reactions in the astrophysical relevant energies.  $^{137}\text{Ce}$  is adjacent to the  $^{136}\text{Ce}$  (0.185% abundance) which is one of the heaviest of the so-called *p* nuclei and is likely formed via successive  $(\gamma, n)$  or a combination of  $(\gamma, n)$  and  $(\gamma, p)$  processes starting from  $^{140}\text{Ce}$  (88.45%) or  $^{141}\text{Pr}$  (100%) seed nuclei. The relative population of the isomer and ground state via  $^{138}\text{Ce}(\gamma, n)$  could affect *p*-process network calculations. Similarly,  $^{84}\text{Sr}$  (0.56%) *p* nuclide can be produced through a combination of  $(\gamma, n)$  and  $(\gamma, p)$  processes starting from  $^{89}\text{Y}$  (100%). Cross section measurements for nuclear reactions, like  $^{136}\text{Ce}(n, \gamma)^{137}\text{Ce}$  and  $^{84}\text{Sr}(p, \gamma)^{85}\text{Y}$ , are measured via the activation technique for nucleosynthesis studies [36,37] and the use of accurate  $\gamma$ -ray emission probability of  $^{137}\text{Ce}^g$  and  $^{85}\text{Y}^g$  is pivotal to provide accurate input data for any subsequent studies. Furthermore, an emerging motivation for more accurate decay data of radionuclides of trivalent metals, like scandium, gallium, yttrium, and rare earths, lies in their use in certain chemical forms as tumor-seeking agents. This characteristic of trivalent metal radionuclides strongly supports the fast developing theranostic approach in nuclear medicine, which involves a combination of diagnosis and internal radiotherapy, specific to a patient [38]. To this aim, use is generally made of a “matched pair” of radionuclides, i.e., a positron-emitting diagnostic radionuclide and a  $\beta^-$ - or  $\alpha$ -emitting therapeutic radionuclide of the same element in the same chemical form. The distribution of the radioactivity in various organs of the body is determined by positron emission tomography (PET) and from the pharmacokinetic data thus obtained the radiation dose through the therapeutic radionuclide is quantified. Several matched pairs of trivalent metals are being developed [38]. One such pair is  $^{86}\text{Y}/^{90}\text{Y}$ , which is commonly used [39]. The reactor-produced  $\beta^-$ -emitting therapeutic radionuclide  $^{90}\text{Y}$  (2.7 d) is commercially available but the production of  $^{86}\text{Y}$  (14.7 h) is carried out at a cyclotron using the reaction  $^{86}\text{Sr}(p, n)^{86}\text{Y}$ . Closely associated with this production route is the nuclear process  $^{86}\text{Sr}(p, 2n)^{85}\text{Y}^{m,g}$ . These two positron-emitting isomers, if present in large quantity, would deteriorate the quality of the

PET scan of  $^{86}\text{Y}$  and would also cause higher uncertainty in dose quantification. On the other hand, they may also replace  $^{86}\text{Y}$  in some special investigations. Obviously, in all those medically oriented studies, the necessity of high-accuracy decay data, including the intensities of all emitted gamma rays, cannot be overemphasized, especially with regard to dose quantification [40].

## II. WORKING EQUATIONS

The radioactivity of a daughter radioisotope  $A_d(t)$  at time  $t$  with an initial activity of  $A_d(0)$  and contributions from a radioactive decay chain of three isotopes,  $X(\text{parent}) \xrightarrow{\lambda_p} Y(\text{daughter}) \xrightarrow{\lambda_d} Z$ , may be obtained from the Bateman equation [41]:

$$A_d(t) = A_p(0) \frac{\lambda_d}{\lambda_d - \lambda_p} \times (e^{-\lambda_p t} - e^{-\lambda_d t}) \times \text{BR} + A_d(0) e^{-\lambda_d t}, \quad (1)$$

where  $A_p(0)$  and  $A_p(t)$  are the radioactivity of the parent at  $t = 0$  and after a decay time  $t$ , respectively;  $\lambda_p$  and  $\lambda_d$  are the decay constants for the parent and daughter nuclides, respectively, and BR is the decay mode branching of the parent. After a decay time  $\geq 10$  half-lives of the daughter, the second term in Eq. (1) becomes negligible and it reduces to

$$A_d(t) = A_p(0) \frac{\lambda_d}{\lambda_d - \lambda_p} \times (e^{-\lambda_p t} - e^{-\lambda_d t}) \times \text{BR}$$

or  $A_d(t) = A_p(t) \frac{\lambda_d}{\lambda_d - \lambda_p} \times (1 - e^{-(\lambda_d - \lambda_p)t}) \times \text{BR}, \quad (2)$

where  $A_p(t) = A_p(0) e^{-\lambda_p t}$ . In equilibrium

$$A_d(t) = A_p(t) \frac{\lambda_d}{\lambda_d - \lambda_p} \times \text{BR}. \quad (3)$$

The time needed,  $t_{\text{max}}$ , to reach the daughter activity to the maximum, i.e., to equilibrium, can be calculated using the following relation:

$$t_{\text{max}} = \frac{1}{\lambda_d - \lambda_p} \ln \frac{\lambda_d}{\lambda_p}, \quad (4)$$

derived solving  $dA_d(t)/dt = 0$  at  $t_{\text{max}}$ ,  $A_d(t)$  in Eq. (2). The radioactivity  $A(t)$  for a parent/daughter may be obtained from the measured  $\gamma$ -ray intensity using the general radioactivity equation:

$$A(t) = \lambda N_t = \frac{\lambda C_n}{P_\gamma \times \varepsilon_\gamma \times (1 - e^{-\lambda t_c})}, \quad (5)$$

where  $N_t$  is the number of radioisotopes at time  $t$ .  $C_n$ ,  $\varepsilon_\gamma$ , and  $P_\gamma$  are the net counts under the peak for a counting period of  $t_c$ , the detector efficiency, and the emission probability for the  $\gamma$  ray of interest, respectively. For a very short counting period  $t_c$  compared to half-life  $T$  of the radioisotope, i.e.,  $0 < t_c \ll T$ , Eq. (5) with one decay constant  $\lambda$ , can be approximated as follows:

$$A(t) \approx \frac{C}{P_\gamma \times \varepsilon_\gamma}, \quad (6)$$

where  $C$  is the net count per second for the  $\gamma$  ray of interest. In the limit of  $t_c < 3\%T$  Eq. (6) yields  $A(t) > 99\%$  compared to that of using Eq. (5). Inserting Eq. (6) in Eq. (3) and rearranging, we obtain the following equation for the  $\gamma$ -ray emission probabilities and relative  $\gamma$ -ray intensities for the parent and daughter radioisotopes:

$$\frac{P_{\gamma p}}{P_{\gamma d}} = \frac{I_{\gamma p}}{I_{\gamma d}} \times \frac{\lambda_d}{\lambda_d - \lambda_p}, \quad (7)$$

where  $P_{\gamma p}$  and  $P_{\gamma d}$  are the  $\gamma$ -ray emission probabilities,  $I_{\gamma p}$  and  $I_{\gamma d}$  are the relative  $\gamma$ -ray intensities of the parent and daughter radioisotopes, respectively, and  $I_\gamma = C/\varepsilon_\gamma$ . Equation (7) can further be simplified replacing the decay constant  $\lambda$  by half-life  $T$  from their relation  $\lambda = \ln(2)/T$  to yield

$$\frac{P_{\gamma p}}{P_{\gamma d}} = \frac{I_{\gamma p}}{I_{\gamma d}} \times \frac{T_p}{T_p - T_d} = \frac{I_{\gamma p}}{I_{\gamma d}} \times F \quad (8)$$

or

$$\frac{P_{\gamma p}}{P_{\gamma d}} = \frac{I_{\gamma p}}{(I_{\gamma d}/F)} = \frac{I_{\gamma p}}{I_{\gamma dc}}, \quad (9)$$

where  $T_p$  and  $T_d$  are the half-lives for parent and daughter radioisotopes, respectively. We denote  $F = \frac{T_p}{T_p - T_d}$  where the right-hand side is defined in Eq. (3) as  $\frac{\lambda_d}{\lambda_d - \lambda_p}$  and  $I_{\gamma dc} = I_{\gamma d}/F$  as the corrected relative  $\gamma$ -ray intensity in transient equilibrium. The factor ‘‘BR’’ in Eq. (1) is associated with the  $\gamma$ -ray emission probability. We have deduced the  $\gamma$ -ray emission probability using either Eqs. (8) or (9). Note that from measurement only the relative  $\gamma$ -ray intensities of parent and daughter, obtained from the same spectrum, are required in Eqs. (8) or (9). As a result, all the systematic uncertainties related to the target, beam current, dead time, counting position, detector efficiency, etc., cancel out.

## III. MEASUREMENTS

The experiments were performed using a proton beam from the 88-in. cyclotron at Lawrence Berkeley National Laboratory (LBNL) on natural lanthanum and thin  $^{86}\text{SrCO}_3$  targets (96.4%  $^{86}\text{Sr}$ ) in order to determine cross sections of interest for medical radioisotope production by activation technique. Here we describe the irradiations and measurements in detail relevant to this work, i.e., for relative  $\gamma$ -ray intensities of the parent and daughter radioisotopes in transient equilibrium. Cross section data of the  $^{139}\text{La}(p, x)$  reactions have been published by Morrell *et al.* [42] and data of the  $^{86}\text{Sr}(p, x)$  reactions will be published in upcoming articles.

### A. Target preparation and irradiation

Natural lanthanum foils of thickness  $\sim 25 \mu\text{m}$  and 99% purity were purchased from GoodFellow USA. These foils, 2.54 by 2.54 cm, were supplied in glass ampoules filled with an inert gas to prevent oxidation. Just before irradiation, the foils were opened, cleaned, weighed, sealed with kapton tapes, and placed in aluminum target frames. A stack of ten lanthanum foils along with copper and aluminum foils was mounted inside a sample holder for irradiation. The stack was irradiated with a 57-MeV proton beam for 1 h and 37 min

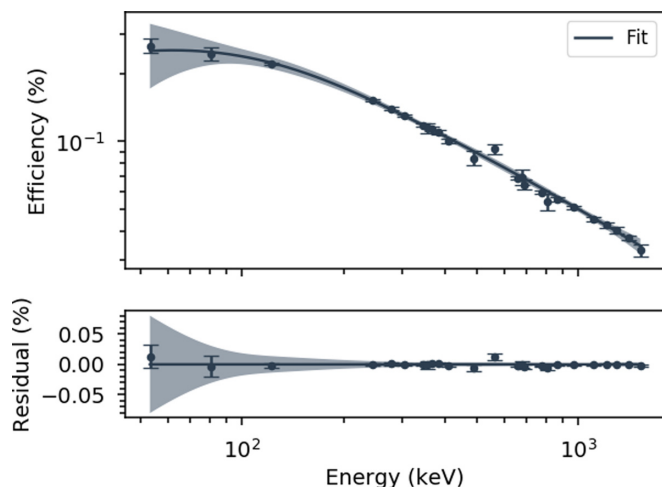


FIG. 2. The measured HPGe detector efficiency at 30 cm (points with uncertainty) along with the fitted line. The shaded region represents the  $1\sigma$  confidence band.

with a beam current of about 8 nA. The radionuclide  $^{137}\text{Ce}^{m,g}$  was produced through the  $^{139}\text{La}(p, 3n)$  reaction. It may be mentioned here that sample no. 3, listed in Table I, was damaged during the irradiation due to oxidation, however, for relative  $\gamma$  ray intensity measurements it was not a problem, as pointed out in Sec. II.

For  $^{85}\text{Yg}$  production, thin  $^{86}\text{SrCO}_3$  targets were prepared via a sedimentation method described in Ref. [43]. The  $^{86}\text{SrCO}_3$  sample enriched to 96.4%  $^{86}\text{Sr}$  was supplied by Eurisotop (France). A stack of eight  $\text{SrCO}_3$  targets along with five copper, six titanium, and three iron foils was mounted inside a sample holder for irradiation. The stack was irradiated with a 27-MeV proton beam for 30 min with a beam current of 150 nA. The radioisotope  $^{85}\text{Yg}$  was produced through the  $^{86}\text{Sr}(p, 2n)$  reaction.

### B. Data acquisition and analysis

After the irradiation, target and monitor foils were counted using a shielded HPGe detector with an ORTEC PC-based acquisition system. The  $\gamma$ -ray energy spectra were collected about 15 min after the end of irradiation and continued for several days for different reaction products based on their half-lives. The energy resolution of the HPGe detector was 4.9 and 2.5 keV full width at half maximum (FWHM) at  $E_\gamma = 1332.5$  keV, achieved using 8 and 16 K channels during Ce and Sr sample counting, respectively. The efficiency of the HPGe detector was measured at different distances from the detector surface using standard  $\gamma$ -ray point sources of  $^{54}\text{Mn}$ ,  $^{137}\text{Cs}$ ,  $^{133}\text{Ba}$ , and  $^{152}\text{Eu}$  purchased from Isotope Products Laboratories. The efficiency for closer counting positions of the detector was obtained by normalizing the efficiency data measured at 30 cm with ratios of single  $\gamma$  lines. Single  $\gamma$  rays of energy 661.4 and 834.8 keV from  $^{137}\text{Cs}$  and  $^{54}\text{Mn}$ , respectively, were used. The measured efficiency at 30 cm from the detector surface is presented in Fig. 2 along with the fitted line produced using the functional form of  $\varepsilon(E) = A * (-b_1 E^{c_1}) * (1 - e^{-b_2 E^{c_2}})$ , where  $A$ ,  $b_1$ ,  $b_2$ ,  $c_1$ , and  $c_2$  are the

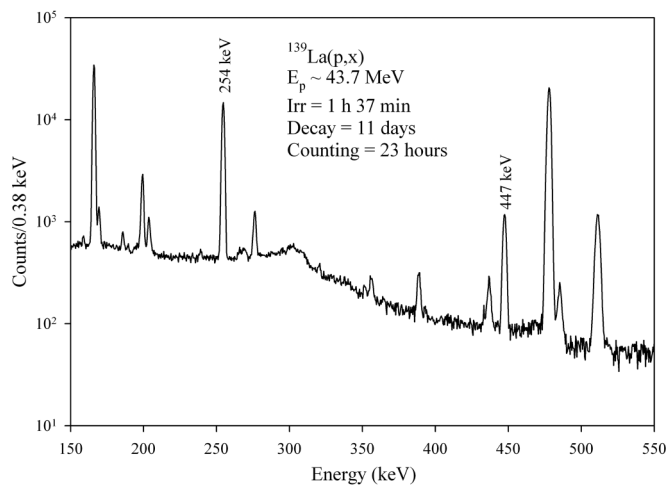


FIG. 3. A partial HPGe  $\gamma$ -ray spectrum of  $^{137}\text{Ce}^g$  (9 h) in transient equilibrium with  $^{137}\text{Ce}^m$  (34.4 h); their corresponding 447- and 254-keV  $\gamma$  rays are labeled.

fitting parameters. The functional form accounts for the dead-layer efficiency dropoff at low (x-ray) energies. The shaded region represents the  $1\sigma$  confidence band on the efficiency data. A few weaker  $^{152}\text{Eu}$   $\gamma$  rays, like 488.1, 564.0, and 810.5 keV with  $P_\gamma < 0.5\%$ , were barely or closely fitted due to lower counting statistics. A residual plot is also presented in Fig. 2. The  $\gamma$ -ray energy spectra for the  $^{137}\text{Ce}^m$  (34.4 h) isomeric decay and  $^{137}\text{Ce}^g$  (9 h) electron capture and  $\beta^+$  decay, collected after a decay time  $> 160$  h, for all ten samples were analyzed. The decay time was more than ten half-lives of  $^{137}\text{Ce}^g$  (9 h), thereby allowing any directly produced  $^{137}\text{Ce}^g$  via the  $^{139}\text{La}(p, 3n)$  reaction to decay away and ensuring that the radioactivity of  $^{137}\text{Ce}^g$  was from the parent  $^{137}\text{Ce}^m$  decay alone. During counting, the daughter radioactivity was in transient equilibrium with the parent. These spectra were collected at 1 cm distance from the detector surface. The summing effect was negligible for counting at this close distance. The 254- and 447-keV  $\gamma$  rays, from the decay of  $^{137}\text{Ce}^m$  and  $^{137}\text{Ce}^g$ , respectively, were well separated from neighboring  $\gamma$ -ray peaks (see Fig. 3) and the net area was obtained using the ORTEC GammaVision Software. It may be mentioned that the population branching of the isomeric and ground state,  $\sigma_{m,g}/(\sigma_m + \sigma_g)$ , in  $^{137}\text{Ce}^{m,g}$  was 78(4) and 22(4)%, respectively, with insignificant variation in the incident proton beam energy range of 36–56 MeV, deduced using the cross section data  $\sigma$  from Ref. [42]. In the  $^{139}\text{La}(p, 3n)$   $^{137}\text{Ce}^{m,g}$  reaction, the high-spin ( $11/2^-$ ) isomeric state was preferentially populated compared to the low-spin ( $3/2^-$ ) ground state due to higher angular momentum of the compound nucleus carried by the high-energy protons. However, for cases with low-energy projectile induced reactions the population branching would be the other way around. For example, in thermal neutron capture reaction,  $^{136}\text{Ce}(n, \gamma) ^{137}\text{Ce}^{m,g}$ , the population branching of the isomeric state was measured to be 8.1(5)% [22].

The  $\gamma$ -ray energy spectra for the  $^{85}\text{Yg}$  (2.68 h) electron capture and positron decay and  $^{85}\text{Sr}^m$  (1.127 h) isomeric decay

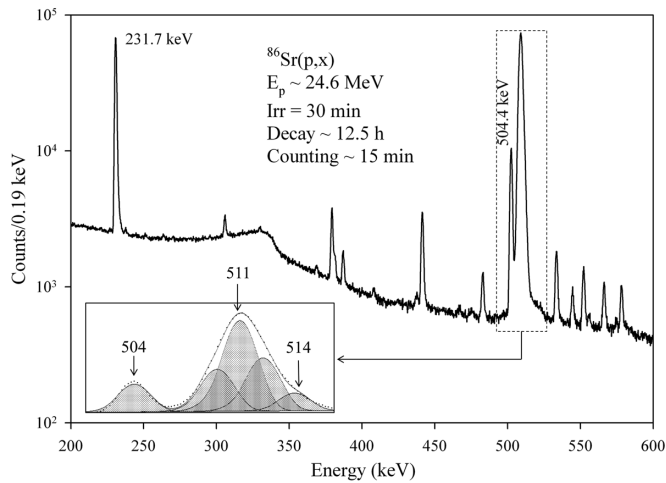


FIG. 4. A partial HPGe  $\gamma$ -ray spectrum in transient equilibrium of  $^{85}\text{Sr}^m$  (1.127 h) with  $^{85}\text{Y}^g$  (2.68 h); their corresponding 232- and 504-keV  $\gamma$  rays are labeled. Inset represents fitted peaks by Fitzpeak gamma analysis software in selected region. 504-keV  $\gamma$  peak separated neatly from the 511-keV annihilation peak. The 514-keV  $\gamma$  peak comes from  $^{85}\text{Sr}$  (64.849 d) decay. The annihilation peak was fitted with three component peaks, 511 (labeled) and two others by the sides, owing to its characteristic broader width compared to other  $\gamma$ -ray peaks, used for FWHM calibration.

(99.21%) were collected at 18 and 11 cm distances from the detector surface considering the detector dead time <25%. Actual dead time was in the range of 14–21%, calculated using the real and live time of the acquisition system. Measurable  $\gamma$  rays from these radioisotopes were detected in the first six out of eight samples in the target stack. The decay time was 12.5, 12.0, 11.7, 9.0, 8.7, and 8.5 h for samples 1–6, respectively, listed in Table II, corresponding to 11.1–7.5 half-lives of  $^{85}\text{Sr}^m$  (1.127 h). The decay time frame allowed us to decay away 99.0–99.9% directly produced  $^{85}\text{Sr}^m$  through the  $^{86}\text{Sr}(p, pn)$  reaction, i.e., the second term of Eq. (1) was negligible. However,  $^{85}\text{Y}^m$  (4.86 h) which has a 100% electron capture and  $\beta^+$  decay branch to  $^{85}\text{Sr}$  was also present in the sample, so another set of  $\gamma$ -ray spectra was collected after a decay time >27 h placing the samples at 10 cm distance from the detector surface. These spectra were used to subtract the contribution of  $^{85}\text{Y}^m$  (4.86 h) from the 232- and 504-keV  $\gamma$  rays of the first set of spectra, which contained the contribution from both the  $^{85}\text{Y}^g$  (2.68 h) and the  $^{85}\text{Y}^m$  (4.86 h) decays. The 504-keV  $\gamma$  ray from  $^{86}\text{Y}^g$  decay was close to the 511-keV annihilation peak (see Fig. 4) and the net peak area was obtained using the FitzPeak gamma analysis software. A partial decay scheme for  $^{85}\text{Sr}$  is presented in Fig. 5 from the  $^{85}\text{Y}^g$  (2.68 h) and  $^{85}\text{Y}^m$  (4.86 h) decay. Full and detailed decay schemes can be found in Ref. [44].

## IV. RESULTS AND DISCUSSION

### A. $^{137}\text{Ce}^g$

The relative  $\gamma$ -ray intensities of 254- and 447-keV  $\gamma$  rays from the decay of  $^{137}\text{Ce}^m$  and  $^{137}\text{Ce}^g$ , respectively, measured

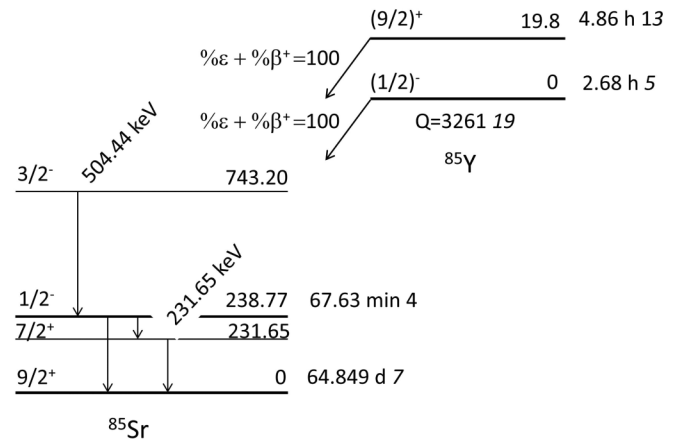


FIG. 5. Partial  $^{85}\text{Sr}$  level scheme (not in scale) from  $^{85}\text{Y}^g$  (2.68 h) and  $^{85}\text{Y}^m$  (4.86 h) decays [44], showing 504- and 232-keV  $\gamma$  rays from the 743- and 232-keV levels, respectively.

in transient equilibrium are presented in Table I. The emission probability  $\%P_\gamma$  for the 447-keV  $\gamma$  ray has been obtained using Eq. (8) and found to be 1.21(3) relative to the emission probability of  $\%P_\gamma(254) = 11.11(15)$ . The  $\%P_\gamma(254)$  value was deduced using isomeric transition branching  $\%IT = 99.21(4)$  [20] and a conversion coefficient  $\alpha$  of 7.93(12) [21] for the 254.29(5)-keV M4 transition in cerium. Our results along with the literature data [9,16–20,22,24,25] are presented in Table I.

From the measured relative  $\gamma$ -ray intensities of 254- and 447-keV transitions, we obtain the ratio  $I_\gamma(254)/I_\gamma(447) = 6.78(9)$ . As can be seen in Table I, this value is comparable with 6.0(6), obtained using the  $I_\gamma$  data reported in Ref. [25]. However, it differs significantly from the value of 4.91(15) reported by Henry *et al.* [9]. The value in Ref. [9] is listed only with the statement “In transient equilibrium spectra  $I(254)/I(447) = 4.91(15)$ ,” making no mention of whether or not the time-dependent factor  $F$  was applied. From half-lives of 34.4(3) and 9.0(3) h for  $^{137}\text{Ce}^m$  and  $^{137}\text{Ce}^g$ , respectively, we obtain the value of time-dependent factor  $F$  as 1.354(17). If we divide our ratio 6.78(9) by the factor  $F$ , we obtain 5.01(9), which is in good agreement with Henry’s value of 4.91(15). It appears that the time-dependent factor was used by Henry *et al.* [9] to divide the ratio of  $I_\gamma(254)/I_\gamma(447)$ . However, it can be seen from Eq. (8) that the intensity ratio  $I_\gamma(254)/I_\gamma(447)$  should have been multiplied instead of dividing by the time-dependent factor.

We have therefore revised the ratio 4.91(15) [9] and using Eq. (8) obtained  $\%P_\gamma(447)$  as 1.23(5). The revised  $\%P_\gamma(447)$  value is in excellent agreement with our measured value of 1.21(3)%. The other  $\%P_\gamma(447) = 1.4(2)$  presented in Table I has been deduced using the data from [25]. This value is statistically consistent with our value 1.21(3) but the central value is higher. It is probably due to insufficient decay time being allotted prior to the collection of the  $\gamma$ -ray spectrum. Beery [25] noted “All relative  $\gamma$  intensities are measured after transient equilibrium has been reached ( $\leq 80$  h after bombardment),” however, the decay time was not given specifically. As mentioned in Sec. III B, a decay time of  $\geq 10$  half-lives

TABLE I. Relative  $I_\gamma(254)$  and  $I_\gamma(447)$  from the decay of  $^{137}\text{Ce}^m$  and  $^{137}\text{Ce}^g$ , respectively, in transient equilibrium, are listed in columns 2 and 3. Ratio =  $I_{\gamma p}/I_{\gamma d}$  and unweighted average in columns 4 and 5, corrected ratio =  $I_{\gamma p}/I_{\gamma d} \times F$  and emission probability of 447-keV  $\gamma$  ray are presented in columns 6 and 7, respectively.  $F = 1.354(17)$ .

Sample no./[Ref.]	$I_{\gamma p}(254)$	$I_{\gamma d}(447)$	$I_{\gamma p}/I_{\gamma d}$	$I_{\gamma p}/I_{\gamma d}$	$I_{\gamma p}/I_{\gamma d} \times F$	$\%P_\gamma(447)$
1	624(9)	100(8)	6.24(51)	6.78(9) <sup>a</sup>	9.18(17)	1.21(3) <sup>b</sup>
2	670(15)	100(7)	6.70(48)			
3	643(12)	100(10)	6.43(65)			
4	723(5)	100(4)	7.23(29)			
5	685(3)	100(2)	6.85(14)			
6	692(3)	100(2)	6.92(14)			
7	684(2)	100(1)	6.84(7)			
8	673(3)	100(2)	6.73(14)			
9	696(1)	100(1)	6.96(7)			
10	687(1)	100(1)	6.87(7)			
[25]	600(40)	100(7) <sup>c</sup>		6.0(6)	8.1(13)	1.4(2) <sup>d</sup>
[9]				4.91(15)		2.24(10)
[16]						2.2(1) <sup>e</sup>
[17] p. 161						2.24(10) <sup>e</sup>
[18]						2.24(10) <sup>e</sup>
[19] p. 836						1.78(8) <sup>f</sup>
[20]						1.68(6) <sup>f</sup>
[22]						1.69
[9] (revised)					9.00(32) <sup>g</sup>	1.23(5) <sup>g</sup>

<sup>a</sup>Unweighted average of ten values presented in column 4.

<sup>b</sup>This work.

<sup>c</sup>100 in Ref. [25], we have assumed 7% uncertainty.

<sup>d</sup>Obtained here using the data from [25]. Using the same data, Bunting [24] (p. 355) proposed 1.4(3).

<sup>e</sup>Same/similar value as that of Ref. [9].

<sup>f</sup>Correcting the ratio 4.91(15) [9] for time dependence, assuming not done by authors.

<sup>g</sup>Revised value using the ratio 4.91(15) [9]; see text for details.

of the daughter is needed to allow complete decay of the directly produced  $^{137}\text{Ce}^g$  through the  $^{139}\text{La}(p, 3n)$  reaction, otherwise, additional counts would be accumulated under the 447-keV  $\gamma$ -ray peak, i.e., the second term in Eq. (1) would not be negligible. This would result in a lower ratio value for  $I_\gamma(254)/I_\gamma(447)$  and thus a higher value for  $\%P_\gamma(447)$ .

Since 1975, the recommended  $\%P_\gamma(447)$  value varied between 2.25(5) and 1.68(6), as presented in Table I. As a result, the accuracy of all the cross section data measured by activation technique was most likely deviated by the same fraction compared to  $\%P_\gamma(447) = 1.21(3)$ , where the reaction product was  $^{137}\text{Ce}^g$ . In many cases, the measured cross section data, especially with an isomeric and ground state pair, have been used for studying the angular momentum effects in nuclear reactions, spin dependence of the nuclear level density [26,29–32], elemental evolution in a stellar environment [22,36,37], and to recommend Maxwellian-averaged ( $n, \gamma$ ) cross sections at thermal energy  $kT = 30$  keV [45]. Existing experimental cross section data if deduced using incorrect  $\%P_\gamma(447)$  should be revised for inclusion as input for further studies. The  $\%P_\gamma(447)$  value of this work will also be useful to normalize the  $^{137}\text{Ce}^g$  decay scheme to provide accurate quantitative intensity data for all related radiations, like  $\beta$ ,  $x$  ray, and all other  $\gamma$  rays, etc.

## B. $^{85}\text{Y}^g$

The relative intensities of the 504- and 232-keV  $\gamma$  rays from the decay of  $^{85}\text{Y}^g$  and  $^{85}\text{Sr}$ , respectively, measured in transient equilibrium, are presented in Table II. The relative intensity  $I_\gamma(232)$  of the daughter has been corrected using the time-dependent factor  $F = 1.73(8)$ . It was calculated using the half-lives of 2.68(5) h and 1.127(67) h for  $^{85}\text{Y}^g$  and  $^{85}\text{Sr}^m$ , respectively. Finally, an unweighted average value of 139(4) was obtained for the time-dependent corrected  $I_\gamma(232)$  and the emission probability of  $\%P_\gamma(504) = 60(2)$  was deduced using  $\%P_\gamma(232) = 83.9(4)$  [44] in Eq. (9). Our value agrees well with the recommended value of 60(5)% [44], however, the uncertainty has been improved from 8.3 to 3.3%. New value would yield more precision to the determination of the absolute activity of  $^{85}\text{Y}^g$  for use in cross section measurements or in other uses.

Liptak *et al.* [6] presented the relative intensity  $I_\gamma(232) = 140(10)$  with respect to  $I_\gamma(504) = 100$ , however, the authors did not mention whether or not the daughter  $I_\gamma(232)$  was corrected for the time-dependent factor. To normalize the  $^{85}\text{Y}^g$  decay scheme, these values were used with the assumption that the value 140(10) was corrected for a time-dependent factor [44]. The assumption was consistently used since the publication of that article, so we find that all the recommended

TABLE II. Relative  $I_\gamma(504)$  and  $I_\gamma(232)$  from the decay of  $^{85}\text{Y}^g$  and  $^{85}\text{Sr}^m$ , respectively, measured in transient equilibrium. Statistical uncertainty of the former  $I_\gamma$  has been propagated with that of the latter one. Corrected  $I_{\gamma dc} = I_{\gamma d}(232)/F$ , unweighted average in columns 4 and 5, and emission probability of 504-keV  $\gamma$  ray are presented in column 6.  $F = 1.73(8)$ .

Sample no./[Ref.]	$I_{\gamma p}(504)$	$I_{\gamma d}(232)$	$I_{\gamma dc}(232)$	$I_{\gamma dc}(232)$	$\%P_\gamma(504)$
1	100	241(2)	139(7)	139(4) <sup>a</sup>	60(2) <sup>b</sup>
2	100	245(2)	142(7)		
3	100	237(2)	137(6)		
4	100	245(2)	142(7)		
5	100	259(3)	150(7)		
6	100	213(5)	123(6)		
[6]	100			140(10)	
[44]					60(5) <sup>c</sup>

<sup>a</sup>Unweighted average of six values presented in column 4.

<sup>b</sup>This work.

<sup>c</sup>Using data from Ref. [6] and assuming that 140(10) was corrected for time dependence by authors.

values over the decades in Refs. [16,18,44,46] are consistent. Our work shows that the assumption is indeed a correct one.

## V. CONCLUSIONS

For the  $^{137}\text{Ce}^g$  decay, the emission probability of the 447-keV  $\gamma$  ray was measured to be 1.21(3)%, which differs significantly from an earlier published value of 2.24(10)% [9]. From our measured data, we show that the discrepancy was caused by the incorrect use of the time-dependent factor in the denominator in Eq. (8) as opposed to the numerator. A revised value of 1.23(5)% was obtained using the datum of Ref. [9]. The revised value is in excellent agreement with our value 1.21(3)%. This work resolves the discrepancy of  $\%P_\gamma(447)$  in  $^{137}\text{Ce}^g$  decay and provide accurate and more precise value compared to earlier data. The new value will yield accurate and more precise cross section data by activation technique for future measurements and will be useful to normalize the  $^{137}\text{Ce}^g$  decay scheme to provide accurate quantitative data for all related radiations, like  $\beta$ , x-ray, and all other  $\gamma$  rays, etc. Since 1975, the recommended  $\%P_\gamma(447)$  value varied between 2.25(5) and 1.68(6), as presented in Table I. As a result, the accuracy of all the cross section data measured by activation technique was most likely deviated by the same fraction compared to  $\%P_\gamma(447) = 1.21(3)$ , where the reaction product was  $^{137}\text{Ce}^g$ . The measured cross section data involving the  $^{137}\text{Ce}^{m,g}$  product are useful for studying the angular momentum effects in nuclear reactions, the spin dependence of the nuclear level density, and to recommend Maxwellian-averaged ( $n, \gamma$ ) cross sections at thermal energy  $kT = 30$  keV for nucleosynthesis studies. Existing experimental cross section data if deduced using incorrect  $\%P_\gamma(447)$  should be revised for inclusion as input for these studies.

For the  $^{85}\text{Y}^g$  decay, the emission probability of the 504-keV  $\gamma$  ray was found to be 60(2)%, which agrees well with the recommended value of 60(5)% [44]. We have obtained relative  $I_\gamma(232) = 139(4)$  correcting with the time-dependent factor  $F$ , which is in good agreement with the reported value of  $I_\gamma(232) = 140(10)$  by Liptak *et al.* [6]. We confirmed that the reported value of  $I_\gamma(232)$  in Ref. [6] was corrected by the time-dependent factor, which was, however, not explicitly mentioned by the authors. Additionally, the uncertainty of  $\%P_\gamma(504) = 60(2)\%$  has been improved compared to 60(5)%, i.e., from 8.3 to 3.3%. The new value would yield more precision to the determination of the absolute activity of  $^{85}\text{Y}^g$  for use in cross section measurements or in other uses.

To deduce  $\gamma$ -ray emission probabilities from relative  $\gamma$ -ray intensities for nuclides in transient equilibrium, the use of a time-dependent factor is important as shown in Eqs. (8) or (9). In cases where the literature data are ambiguous on the use of time-dependent factor, new experiments are needed to verify the accuracy of the  $\gamma$ -ray emission probabilities. Our work highlights the necessity of explicit description by authors of any time-dependent correction they have made when reporting  $\gamma$ -ray intensities for nuclides in transient equilibrium.

## ACKNOWLEDGMENTS

The authors wish to thank the reviewer for several useful comments and suggestions regarding the manuscript. We wish to express our gratitude to B. Ninemire, N. Brickner, T. Gimpel, and S. Small for their support during experimental setup and for the 88-in. cyclotron operations. We thank S. Spellerberg and K. Giesen (FZJ) for preparing the  $^{86}\text{SrCO}_3$  samples. This work was performed under the auspices of the US Department of Energy by Lawrence Berkeley National Laboratory under Contracts No. LAB16-1588 NSD and No. DE-AC02-05CH11231.

[1] N. Marnada, H. Miyahara, N. Ueda, K. Ikeda, and N. Hayashi, *Nucl. Instrum. Methods Phys. Res. A* **480**, 591 (2002).

[2] U. Schötzig, *Nucl. Instrum. Methods Phys. Res. A* **286**, 523 (1990).



- [3] D. Pérez-Loureiro, C. Wrede, M. B. Bennett, S. N. Liddick, A. Bowe, B. A. Brown, A. A. Chen, K. A. Chipps, N. Cooper, D. Irvine, E. McNeice, F. Montes, F. Naqvi, R. Ortez, S. D. Pain, J. Pereira, C. J. Prokop, J. Quaglia, S. J. Quinn, J. Sakstrup *et al.*, *Phys. Rev. C* **93**, 064320 (2016).
- [4] J. C. Thomas, L. Achouri, J. Aysto, R. Beraud, B. Blank, G. Canchel, S. Czajkowski, P. Dendooven, A. Ensalle, J. Giovinazzo, N. Guillet, J. Honkanen, A. Jokinen, A. Laird, M. Lewitowicz, C. Longour, F. de Oliveira Santos, K. Perajarvi, and M. Stanoiu, *Eur. Phys. J. A* **21**, 419 (2004).
- [5] K. Ahlgren and P. J. Daly, *Nucl. Phys. A* **189**, 368 (1972).
- [6] J. Lipták, G. Beyer, K. J. Gromov, V. I. Fominikh, A. F. Novgorodov, K. Křišťáková, and W. Habenicht, *Nucl. Phys. A* **256**, 205 (1976).
- [7] S. M. Qaim, T. Bisinger, K. Hilgers, D. Nayak, and H. H. Coenen, *Radiochim. Acta* **95**, 67 (2007).
- [8] M. S. Basunia, *Nucl. Data Sheets* **110**, 999 (2009).
- [9] E. A. Henry, N. Smith, P. G. Johnson, and R. A. Meyer, *Phys. Rev. C* **12**, 1314 (1975).
- [10] J. I. Prisciandaro, A. C. Morton, and P. F. Mantica, *Nucl. Instrum. Methods Phys. Res. A* **505**, 140 (2003).
- [11] N. Larson, S. N. Liddick, M. Bennett, A. Bowe, A. Chemey, C. Prokop, A. Simon, A. Spyrou, S. Suchyta, S. J. Quinn, S. L. Tabor, P. L. Tai, V. Tripathi, and J. M. VonMoss, *Nucl. Instrum. Methods Phys. Res. A* **727**, 59 (2013).
- [12] M. A. Famiano, Y. Nishi, S. Nishimura, and I. Tanihata, *Nucl. Instrum. Methods Phys. Res. A* **496**, 248 (2003).
- [13] C. J. Griffin, T. Davinson, A. Estrade, D. Braga, I. Burrows, P. Coleman-Smith, T. Grahn, A. Grant, L. J. Harkness-Brennan, M. Kogimtzis, I. Lazarus, S. Letts, Z. Liu, G. Lorusso, K. Matsui, S. Nishimura, R. D. Page, M. Prydderch, V. Pucknell, S. Rinta-Antila *et al.*, in *Proceedings of Science, XIII Nuclei in the Cosmos*, edited by Z. Elekes and Z. Fülöp (Debrecen, Hungary, 2016), p. 097.
- [14] R. Caballero-Folch, C. Domingo-Pardo, J. Agramunt, A. Algora, F. Ameil, Y. Ayyad, J. Benlliure, M. Bowry, F. Calviño, D. Cano-Ott, G. Cortès, T. Davinson, I. Dillmann, A. Estrade, A. Evdokimov, T. Faestermann, F. Farinon, D. Galaviz, A. R. García, H. Geissel *et al.*, *Phys. Rev. C* **95**, 064322 (2017).
- [15] S. Nishimura, *Prog. Theor. Exp. Phys.* **2012**, 03C006 (2012).
- [16] *Table of Isotopes*, 7th ed., edited by C. M. Lederer and V. S. Shirley (John Wiley & Sons, New York, 1978).
- [17] L. K. Peker, *Nucl. Data Sheets* **38**, 87 (1983).
- [18] *Table of Radioactive Isotopes*, edited by V. S. Shirley (John Wiley & Sons, New York, 1986).
- [19] L. K. Peker, *Nucl. Data Sheets* **59**, 767 (1990).
- [20] E. Browne and J. K. Tuli, *Nucl. Data Sheets* **108**, 2173 (2007).
- [21] T. Kibédi, T. W. Burrows, M. B. Trzhaskovskaya, P. M. Davidson, and C. W. Nestor Jr., *Nucl. Instrum. Methods Phys. Res. A* **589**, 202 (2008); <http://bricc.anu.edu.au/>
- [22] S. Torrel and K. S. Krane, *Phys. Rev. C* **86**, 034340 (2012).
- [23] Summary Report of an IAEA Technical Meeting, INDC(NDS)-0783, July 2019; <https://www-nds.iaea.org/publications/indc/indc-nds-0783.pdf>
- [24] R. L. Bunting, *Nucl. Data Sheets* **15**, 335 (1975).
- [25] D. B. Beery, Ph.D. thesis, Michigan State University, 1969; [https://groups.nslc.msu.edu/nslc\\_library/Thesis/Beery,%20Dwight.pdf](https://groups.nslc.msu.edu/nslc_library/Thesis/Beery,%20Dwight.pdf)
- [26] D. E. DiGregorio, K. T. Lesko, B. A. Harmon, E. B. Norman, J. Pouliot, B. Sur, Y. Chan, and R. G. Stokstad, *Phys. Rev. C* **42**, 2108 (1990).
- [27] M. S. Rahman, K. S. Kim, M. W. Lee, G. N. Kim, V. D. Nguyen, P. D. Khue, M. H. Cho, and W. Namkung, *J. Kor. Phys. Soc.* **59**, 1749 (2011).
- [28] J. Luo, L. An, and L. Jiang, *Radiochim. Acta* **103**, 613 (2015).
- [29] S. Sudár and S. M. Qaim, *Nucl. Phys. A* **979**, 113 (2018).
- [30] S. Sudár and S. M. Qaim, *Phys. Rev. C* **73**, 034613 (2006).
- [31] N. Chakravarty, P. K. Sarkar, and S. Ghosh, *Phys. Rev. C* **45**, 1171 (1992).
- [32] S. M. Qaim, A. Mushtaq, and M. Uhl, *Phys. Rev. C* **38**, 645 (1988).
- [33] E. M. Burbidge, G. R. Burbidge, W. A. Fowler, and F. Hoyle, *Rev. Mod. Phys.* **29**, 547 (1957).
- [34] S. E. Woosley and W. M. Howard, *Astrophys. J. Suppl.* **36**, 285 (1978).
- [35] T. Rauscher, *Phys. Rev. C* **73**, 015804 (2006).
- [36] F. Käppeler, K. A. Toukan, M. Schumann, and A. Mengoni, *Phys. Rev. C* **53**, 1397 (1996).
- [37] Gy. Gyürky, E. Somorjai, Zs. Fülöp, S. Harissopulos, P. Demetriou, and T. Rauscher, *Phys. Rev. C* **64**, 065803 (2001).
- [38] S. M. Qaim, B. Scholten, and B. Neumaier, *J. Radioanal. Nucl. Chem.* **318**, 1493 (2018).
- [39] F. Rösch, H. Herzog, and S. M. Qaim, *Pharmaceuticals* **10**, 56 (2017).
- [40] S. M. Qaim, *Nucl. Med. Biol.* **44**, 31 (2017).
- [41] H. Bateman, in *Proceedings of the Cambridge Philosophical Society*, Mathematical and physical sciences, Vol. 15, p. 423 (1910).
- [42] J. T. Morrell, A. S. Voyles, M. S. Basunia, J. C. Batchelder, E. F. Matthews, and L. A. Bernstein, *Eur. Phys. J. A* **56**, 13 (2020).
- [43] F. Rösch, S. M. Qaim, and G. Stöcklin, *Radiochim. Acta* **61**, 1 (1993).
- [44] B. Singh and J. Chen, *Nucl. Data Sheets* **116**, 1 (2014).
- [45] Z. Y. Bao, H. Beer, F. Käppeler, F. Voss, K. Wisshak, and T. Rauscher, *At. Data Nucl. Data Tables* **76**, 70 (2000).
- [46] J. W. Tepel, *Nucl. Data Sheets* **30**, 501 (1980).